

A Hybrid-Integrated Artificial Mechanoreceptor in 180nm CMOS

Han Hao¹, Lin Du, Andrew G. Richardson, Timothy H. Lucas, Mark G. Allen, Jan Van der Spiegel, and Firooz Aflatouni²

University of Pennsylvania, Philadelphia, USA

¹hanhao@seas.upenn.edu, ²firooz@seas.upenn.edu

Abstract—A low-power wireless chip for an implantable tactile sensor system is presented. The reported ASIC utilizes the low-loss magnetic human body communication channel for both wireless powering and data transfer. The chip is hybrid-integrated with an in-house fabricated MEMS capacitive force sensor to form an implantable artificial mechanoreceptor (IAM). An on-chip correlated double sampling capacitance-to-time converter consumes $3.9\mu\text{W}$ from a 1.2V on-chip regulated supply and achieves a resolution of 22.8fF over an input capacitance range of 100pF , while occupying an area of only 0.04mm^2 . A wireless power management feedback system is used to ensure robust operation for different hand gestures and under process-voltage-temperature (PVT) variations. The IAM can operate in on-off keying (OOK) or frequency-shift keying (FSK) modulation formats, where the transmitter consumes only $15.6\mu\text{W}$ in OOK mode and is more immune to hand gesture variations in FSK mode. The 1.62mm^2 chip is fabricated in a standard 180nm CMOS process and consumes $104.3\mu\text{W}$.

Keywords—body area network (BAN), capacitance to time converter (CTC), correlated double sampling (CDS), magnetic human body communication (mHBC), power management, sensor interface.

I. INTRODUCTION

Several medical conditions (e.g. paralysis, large-fiber neuropathies) led to irreversible damage of the neural pathways that convey the sense of touch to the brain. This results in numbness of the effected skin, often on the hands. To restore the sense of touch, a sensor-brain interface system could acquire tactile signals and write the information into the brain using a neural stimulator [1]. To acquire the tactile signals, we propose an implantable artificial mechanoreceptor (IAM), composed of a MEMS capacitive force sensor and an interface IC (Fig. 1). The IAM is wirelessly powered and communicates with a base unit worn on the wrist, the wrist device, through a body area network (BAN). In turn, the wrist device could communicate wirelessly with a neural stimulator. Compared to other solutions such as a sensorized glove, this device would not confine hand movement and would be essentially transparent to the user.

Considering the distance and relative orientation between the wrist device and the IAM, the BAN path loss could be excessive reducing the wrist device battery life. Furthermore, any environmental and hand gesture change would potentially lead to a considerable path loss variation interrupting the communication and powering process. Since biological tissues allow magnetic field to travel freely, in this work, we used magnetic human body communication (mHBC) [2], [3], to significantly reduce the path loss compared to galvanic or capacitive electric field human body communication (eHBC),

while maintaining low sensitivity to environmental and gesture change. The mHBC link is formed by incorporating the primary coil in the wrist device and integrating the secondary coil with the IAM. In addition, to compensate for the effect of gesture change as well as process-voltage-temperature (PVT) variations, a wireless power management feedback system is implemented that monitors the received power at the IAM, and dynamically adjusts the transmitted power of the wrist device to ensure uninterrupted sensing and communication at the lowest possible power consumption.

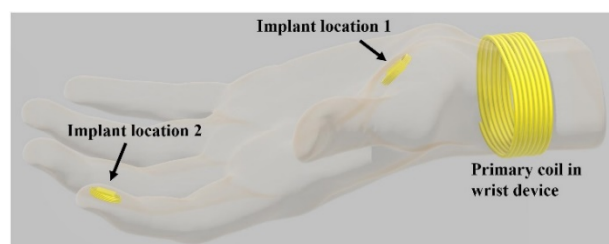


Fig. 1. An implantable tactile sensor system.

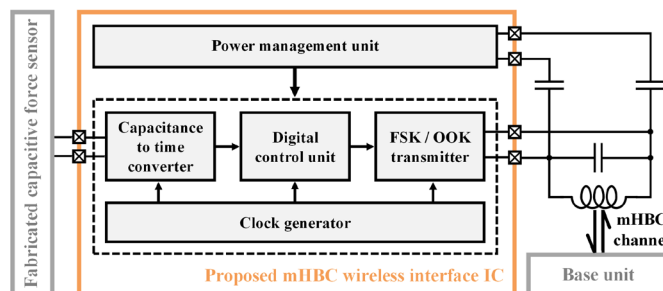


Fig. 2. The block diagram of the implantable artificial mechanoreceptor.

The implemented system both powers and transmits data using mHBC for the first time, with a single coil in the IAM. Fig. 2 shows the block diagram of the implemented IAM, which consists of an in-house fabricated capacitive force sensor and a CMOS chip serving as the interface between the force sensor and the wrist device. The chip consists of a power management unit (PMU), a capacitance to time converter (CTC), a clock generator, a digital control unit (DCU), and the data transmitter (TX). The PMU rectifies the received 7MHz signal and provides regulated voltage supplies for other blocks. It also monitors the IAM input power level, which is then used in the wireless power measurement feedback system to compensate for the gesture change and PVT variations. The CTC uses correlated double sampling (CDS) to cancel the capacitance uncertainty caused by PVT variations, achieving a resolution of 22.8fF over a 100pF input capacitance range. The 10MHz TX

module in IAM can be configured to operate in frequency-shift keying (FSK) or on-off keying (OOK) modes and consumes only 15.6 μ W in the OOK mode.

II. SYSTEM IMPLEMENTATION

A. Power management unit

Fig. 3 shows the schematic of the PMU, which consists of a voltage doubler rectifier, a current mode bandgap reference (BGR), two voltage regulators, and a pair of input power monitors. The rectifier converts the received mHBC power to a DC signal using a full-wave passive structure. To improve the power conversion efficiency (PCE), the diodes are implemented as diode-connected NMOS devices with a near zero threshold voltage. To suppress the output ripple, a larger than 1nF bypass capacitor, C_{BP1} , is implemented using stacked MOS and MIM capacitors for area saving purposes. The simulated rectifier PCE and ripple voltage at an input power of 500 μ W and a load resistance of 10k Ω are 71.7% and 5.5mV, respectively.

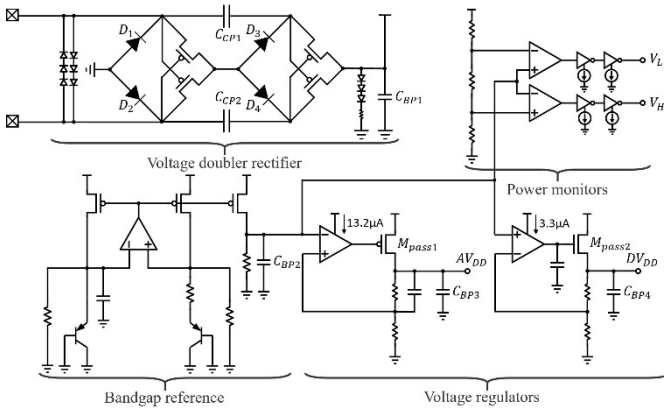


Fig. 3. Schematic of the power management unit.

Two voltage regulators are used to generate separate 1.2V supplies for analog and digital blocks (AV_{DD} and DV_{DD}). For the AV_{DD} regulator, the dominant pole is placed at the regulator output. For the DV_{DD} regulator, the dominant pole is placed at the output of the op-amp. As a result, the AV_{DD} regulator has a higher loop gain and a better line regulation, while the DV_{DD} regulator is more power efficient, has a better load regulation, and remains stable with small load resistance. The bypass capacitors for the BGR and regulators (C_{BP2} to C_{BP4}) are implemented as stacked MOS and MIM capacitors.

To maintain a proper input power level under hand gesture and PVT variations, a closed-loop power management system was utilized [4], [5], where a pair of power monitors are used to compare the divided version of the rectifier output with the BGR output. The generated feedback signals are then wirelessly transmitted to the wrist device to adjust the radiated power accordingly.

B. Correlated double sampling capacitance to time converter

The proposed chip uses a CTC (Fig. 4) to convert the capacitance of the force sensor to a pulse width modulated (PWM) signal, V_{PWM} . The relaxation oscillator-based CTC is

essentially a time-domain correlated double sampler, which alternatively charges an on-chip reference capacitor, C_{ref} , and the sensor capacitor, C_x , to the same threshold voltage. As a result, C_x can be calculated as:

$$C_x = T_x/T_{ref} \times C_{ref}, \quad (1)$$

where T_x and T_{ref} are the time used to charge C_{ref} and C_x , respectively. The CDS technique is used to suppress any capacitance uncertainty caused by PVT variations and low frequency noise. Note that in the proposed CTC design, the oscillation frequency of the relaxation oscillator changes with the input capacitance effectively changing the CTC sampling rate.

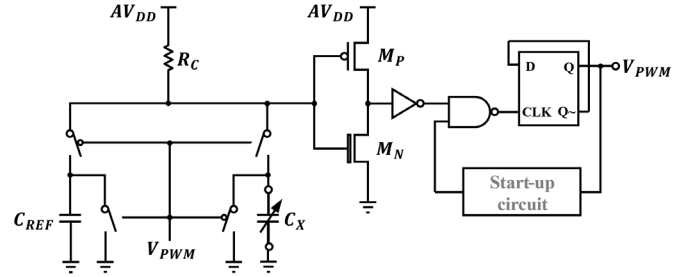


Fig. 4. Schematic of the capacitance to time converter.

C. Timing diagram

Fig. 5 shows the timing diagram of the IAM. The clock signals are generated on-chip using a 40MHz relaxation oscillator (biased using AV_{DD}) followed by a chain of frequency dividers (biased using DV_{DD}). The 40MHz clock drives two 14-bit counters to quantize the CTC output. Data transmission is completed during T_{ref} , since its length depends on C_{ref} and thus remains nearly constant. Triggered by every falling edge of V_{PWM} , a 33-bit output data frame is transmitted, which consists of a 1-bit flag, a 2-bit power monitor output, a 2-bit CTC channel number (reserved for multi-channel measurements, which is not used here), and two 14-bit segments representing T_{ref} and T_x . Each output bitstream requires 27 μ s to be transmitted, which is approximately half the length of T_{ref} .

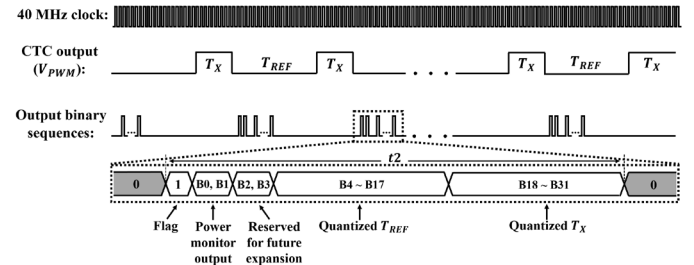


Fig. 5. Chip timing diagram.

D. Digital control unit and transmitter

Fig. 6 shows the simplified schematic of the DCU and TX. The DCU generates the output data by quantizing T_{ref} and T_x alternatively and loading the results into a shift register, which also stores the power monitor output. Controlled by the CTC output, the data will be shifted out to the TX at a rate of

1.25Mbps. The “write enable” and reset signals of the shift register (not shown in Fig. 6), as well as the reset signal of the counters, are generated based on the CTC output and carefully defined time delays.

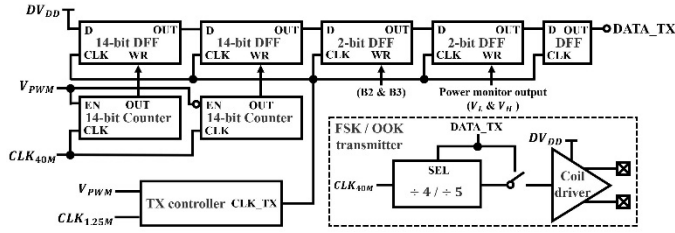


Fig. 6. Simplified schematic of the digital control unit and the transmitter.

Since the signal phase within the mHBC channel strongly depends on the gesture, it is not desirable to employ phase-based modulation schemes [3]. Therefore, the TX of the proposed system is designed to be configurable as either OOK or FSK formats. In the FSK mode, the 40MHz clock is first digitally divided by 4 (logic 0) or 5 (logic 1) and then sent to a coil driver. In the OOK mode, the 40MHz clock is divided by 4 and intermittently sent to the coil driver, which is controlled by the output data. The coil driver consists of a simple single transistor structure. The ultra-low path loss of the mHBC channel allows the TX power to be minimized. In the OOK mode, the TX consumes an average power of only 15.6 μ W.

III. EXPERIMENTAL RESULTS

A. Chip implementation result

The proposed mHBC wireless IC is fabricated in a standard 180nm CMOS process. Fig. 7(a) shows the die microphotograph. The chip area (including bonding pads) is 1.62mm². Fig. 7(b) shows the power breakdown of the chip, with a total power consumption of 104.3 μ W. Fig. 8 shows the chip characterization results in a wireless set-up (coupling through air), where a single coil is used in the IAM for both powering and data transfer. The measured capacitance (the chip output) and the CTC oscillation frequency (*i.e.* the CTC sampling frequency) is shown as the input capacitance, C_x , is varied. Table 1 compares the performance of the proposed CTC with other works.

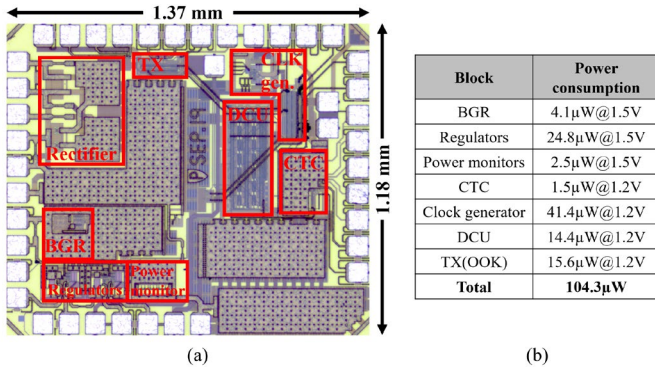


Fig. 7. (a) Die microphotograph. (b) Chip power breakdown.

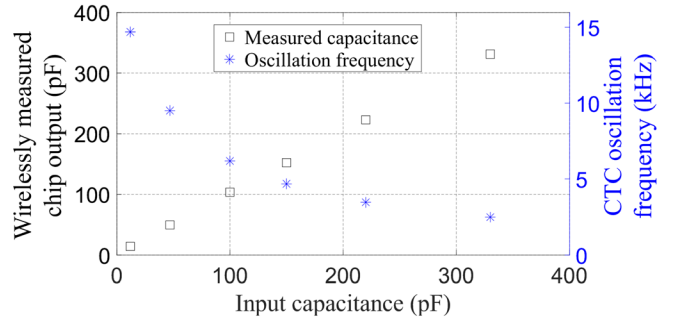


Fig. 8. The measured capacitance (chip output) and CTC oscillation frequency for different input capacitor values.

Table 1. CTC Performance Comparison with other works

Ref.	Process	Area (mm ²)	Cap. Range	Meas. Time	Resolution (fF_{rms})	Power (μ W)
[6] CICC'17	180nm	0.42	10pF	125 μ s	0.4	50.4
[7] ISSCC'19	40nm	0.06	5pF	12.5 μ s	0.29	3.32
[8] JSSC'19	180nm	0.76	17.1pF	850 μ s	1.24	3.09
This work	180nm	0.04	100pF	132μs	22.8^{a,b} 7.2^{a,c}	3.90^b 1.50^c

^a Measured with battery powering;

^b Measured using an on-chip quantizer; ^c Measured using an off-chip quantizer.

B. Measurements with in-house fabricated capacitive force sensor

The chip is characterized using an in-house fabricated capacitive force sensor (Fig. 9, bottom right). The sensor consists of a circular electrode at the bottom of the cavity in the top diaphragm and two semicircular electrodes on the top of the bottom substrate. Therefore, the resulting two capacitors are connected in series by the top electrode. The top diaphragm is fabricated by depositing a patterned thin film of titanium in a dry etching circular cavity inside a fused silica wafer. The substrate silica wafer is packaged with a patterned titanium thin film, and copper electroplated feedthroughs and pads. When there is a normal force applied in the middle of the top diaphragm, the deflection of this top diaphragm induces a decrease of the distance between the top and the bottom electrodes. As a result, the capacitance of the two serial capacitors increases proportional to the normal load applied.

The chip is connected to the sensor through bond wires and PCB traces. A Bose ElectroForce 3200 load frame system is used to characterize the system for different applied normal forces. As shown in Fig. 9, the measured rate of sensor capacitance change with applied force decreases at higher forces due to the flexibility of the diaphragm.

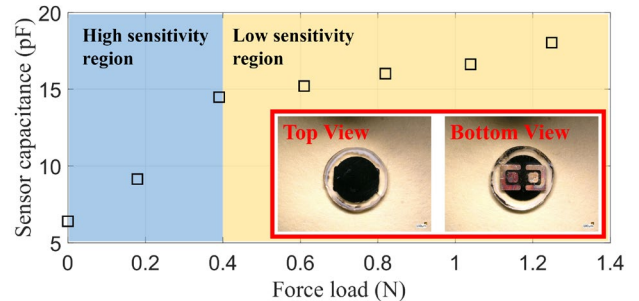


Fig. 9. Fabricated capacitive force sensor and characterizing results using the proposed chip.

Table 2. Performance comparison with prior works.

Ref.	Application	Power link / frequency band	Data link / frequency band	V_{DD} (V)	Chip Power consumption (μ W)	Modulation scheme	TX power (μ W)	Chip area (mm^2)	Process (nm)
[4] JSSC'09	Blood pressure sensing	Inductive coupling / 4MHz	RF telemetry / 433MHz	2	300	FSK	240	4.84	1500
[5] ISSCC'10	Neural recording	Inductive coupling / 13.56MHz	RF telemetry / 915MHz	3	5800	FSK	3300	16.17	5000
[9] JSSC'18	Pressure sensing	Ultrasonic / 790kHz	Ultrasonic / 790kHz	1.9	900	OOK	100	1.767	180
This work	Tactile sensing	mHBC / 7MHz	mHBC / 10MHz	1.2	104.3	FSK / OOK	15.6	1.62	180

C. Wireless demonstration



Fig. 10. Chip measurement setup in a wearable wireless system.

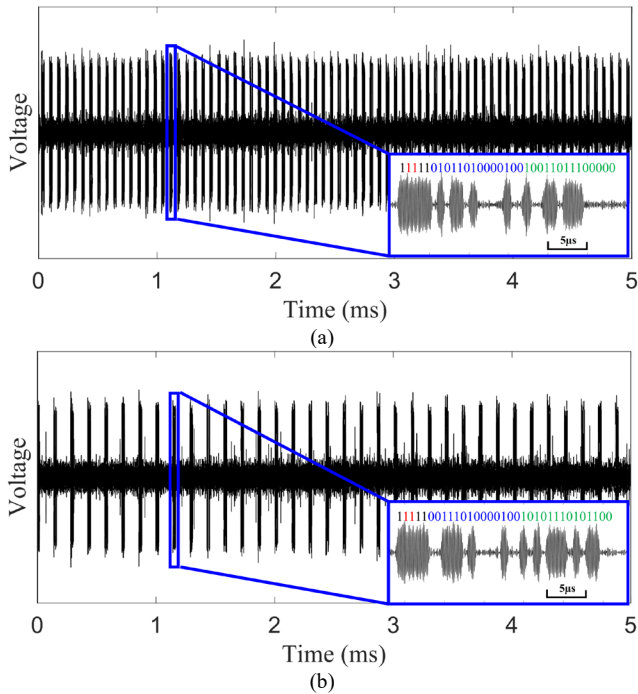


Fig. 11. Received OOK waveforms when the input capacitance is (a) 10pF and (b) 80pF.

The performance of the proposed mHBC wireless IC is measured in a wearable system (Fig. 10), where different values of input capacitors (emulating the force sensor) are used. The chip, together with 2 DC blocking capacitors, a capacitor for impedance matching, and the test capacitor, are mounted on top of a $1\text{cm} \times 1\text{cm}$ printed circuit board (PCB), where a coil is implemented on the back side of the PCB. The PCB is attached to the surface of the skin. A wrist device PCB with a power

amplifier (for power transfer) as well as a low noise amplifier and a notch filter (in the receive path) is designed. Two custom coils made using 24 AWG magnetic wires are used as the power radiator (worn on the wrist) and data receiver (worn on the little finger), respectively. Note that a single coil can also be used for both powering and data transmission (Fig. 8). The mHBC power and data links are frequency multiplexed to 7MHz and 10MHz, respectively. Fig. 11 shows the received OOK waveforms at the wrist device for different input capacitors. Table 2 compares the performance of the implemented IAM with a few previously published works.

ACKNOWLEDGMENT

This work was supported by NIH under grant number 1R01NS107550-01A1.

REFERENCES

- [1] S.N. Flesher, J.L. Collinger, S.T. Foldes, J.M. Weiss, J.E. Downey, E.C. Tyler-Kabara, S.J. Bensmaia, A.B. Schwartz, M.L. Boninger, and R.A. Gaunt, "Intracortical microstimulation of human somatosensory cortex," *Science Translational Medicine*, vol. 8, no. 361, pp. 1-10, October 2016.
- [2] J. Park and P. P. Mercier, "Magnetic human body communication," *2015 37th Annual International Conference of the IEEE Engineering in Medicine and Biology Society (EMBC)*, Milan, 2015, pp. 1841-1844.
- [3] J. Park and P. P. Mercier, "A Sub-10-pJ/bit 5-Mb/s Magnetic Human Body Communication Transceiver," in *IEEE Journal of Solid-State Circuits*, vol. 54, no. 11, pp. 3031-3042, Nov. 2019.
- [4] P. Cong, N. Chaimanonart, W. H. Ko and D. J. Young, "A Wireless and Batteryless 10-Bit Implantable Blood Pressure Sensing Microsystem With Adaptive RF Powering for Real-Time Laboratory Mice Monitoring," in *IEEE Journal of Solid-State Circuits*, vol. 44, no. 12, pp. 3631-3644, Dec. 2009.
- [5] S. B. Lee, H. Lee, M. Kiani, U. Jow and M. Ghovanloo, "An inductively powered scalable 32-channel wireless neural recording system-on-a-chip for neuroscience applications," *2010 IEEE International Solid-State Circuits Conference - (ISSCC)*, San Francisco, CA, 2010, pp. 120-121.
- [6] N. Narasimman, D. Nag, K. C. T. Chuan and T. T. Kim, "A 1.2 V, 0.84 pJ/conv.-Step ultra-low power capacitance to digital converter for microphone based auscultation," *2017 IEEE Custom Integrated Circuits Conference (CICC)*, Austin, TX, 2017, pp. 1-4.
- [7] X. Tang *et al.*, "18.2 A 16fJ/Conversion-Step Time-Domain Two-Step Capacitance-to-Digital Converter," *2019 IEEE International Solid-State Circuits Conference - (ISSCC)*, San Francisco, CA, USA, 2019, pp. 296-297.
- [8] S. Park, G. Lee and S. Cho, "A 2.92- μ W Capacitance-to-Digital Converter With Differential Bondwire Accelerometer, On-Chip Air Pressure, and Humidity Sensor in 0.18- μ m CMOS," in *IEEE Journal of Solid-State Circuits*, vol. 54, no. 10, pp. 2845-2856, Oct. 2019.
- [9] M. J. Weber, Y. Yoshihara, A. Sawaby, J. Charthad, T. C. Chang and A. Arbabian, "A Miniaturized Single-Transducer Implantable Pressure Sensor With Time-Multiplexed Ultrasonic Data and Power Links," in *IEEE Journal of Solid-State Circuits*, vol. 53, no. 4, pp. 1089-1101, April 2018.